ELSEVIER

Quaternary Science Reviews 23 (2004) 1879–1890

QSR

Are the 41 kyr glacial oscillations a linear response to Milankovitch forcing?

Yosef Ashkenazy[a,*], Eli Tziperman[b]

[a]Environmental Sciences, Weizmann Institute, Rehovot 76100, Israel
[b]Department of Earth and Planetary Sciences and Division of Engineering and Applied Sciences, Harvard University, Cambridge, MA, USA

Received 7 January 2004; accepted 20 April 2004

Abstract

The characteristics of glacial oscillations changed drastically ~ 0.8 Ma ago, at the "mid-Pleistocene transition". During the past 0.8 Ma the ~ 100 kyr glacial–interglacial oscillations were strongly asymmetric (i.e., long glacial intervals of growth followed by rapid intervals of deglaciation). The 40 kyr oscillations prior to the mid-Pleistocene transition were of a smaller amplitude and less-asymmetrical looking. The smaller amplitude, apparently symmetric form and period that matches that of obliquity, suggests that these oscillations were a linear response to Milankovitch forcing, while the 100 kyr oscillations are attributed either to some nonlinear self-sustained variability due to a mechanism internal to the climate system itself or to nonlinear amplification of the insolation forcing. The significant strengthening of the 100 kyr eccentricity power in the past ~ 800 kyr is one of the intriguing questions of climate history.

Here we show that glacial–interglacial oscillations pre-mid-Pleistocene transition are, in fact, significantly asymmetric. This asymmetry may contradict a straight forward linear Milankovitch explanation, and we therefore suggest that the glacial oscillations before and after the transition may both be explained as self-sustained variability (although the possibility of nonlinear response to insolation forcing still exists). The role of Milankovitch forcing is in setting the phase of the oscillations (e.g. time of terminations) and their period, rather in being the main driving force of the oscillations. This is demonstrated using a simple model based on the sea ice switch mechanism of Gildor and Tziperman (Paleoceanography 15 (2000) 605).

1. Introduction

Earth climate of the last 2.7 million years (2.7 Ma) was dominated by repetitive and drastic glacial–interglacial oscillations, the ice-ages. These cycles were characterized by a 100 kyr period during the past 0.8 Ma (time of the mid-Pleistocene transition), and by a 40 kyr period before that (Fig. 1). It is generally believed that orbital forcing plays a significant role in this variability (Milankovitch hypothesis), although what that role is still somewhat unclear. Orbital changes occur due to changes in eccentricity (100 kyr time scale), obliquity (40 kyr), and precession (20 kyr) (Milankovitch, 1941; Paillard, 2001). The extreme scenario that eccentricity variations on 100 kyr are responsible for the existence of 100 kyr signal during the past 0.8 Ma is not likely to be valid due to the weak power of eccentricity changes. It is more likely that the 100 kyr oscillations resulted from an internal variability of the climate system (although see Hagelberg et al., 1991) while obliquity and precession variations phase lock (and modulate) the 100 kyr cycles. By phase locking it is meant that the timing of the terminations is set by the Milankovitch forcing. More precisely, one may view the Milankovitch forcing as an external clock felt by the climate system. The 100 kyr oscillations are then weakly influenced by this external clock, and adjust their timing

*Corresponding author. Tel.: +972-8-934-4924; fax: +972-8-934-4124.
E-mail addresses: yossi.ashkenazy@weizmann.ac.il (Y. Ashkenazy), eli@eps.harvard.edu (E. Tziperman).

0277-3791/$ - see front matter © 2004 Elsevier Ltd. All rights reserved.
doi:10.1016/j.quascirev.2004.04.008

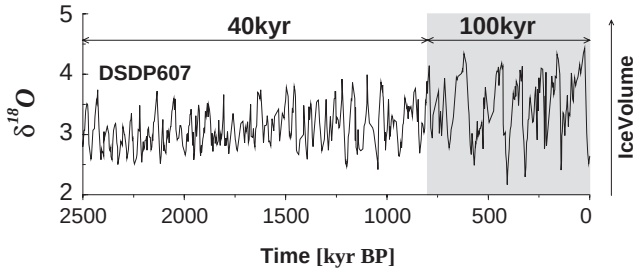

Fig. 1. A typical record of benthic Foraminifera $\delta^{18}O$ (Deep Sea Drilling Project (DSDP) Site 607, Raymo et al., 1989; Ruddiman et al., 1989) which is (at least partly) a proxy for global ice-volume; the record is not orbitally tuned and the chronology is based on the assumption of constant sedimentation rates between several magnetic reversals (see Raymo and Nisancioglu, 2003). While the time period between 2.5 and 0.8 Ma ago is characterized by frequent, less dominant, and more symmetric ice-ages of ~ 40 kyr, the last 0.8 Ma are characterized by less frequent, more pronounced, and more asymmetric ice-ages.

to be in phase with the changes in solar radiation. In addition to the pronounced 1/100 kyr frequency that exists in the power spectrum of the past 0.8 Ma, there are secondary frequencies of 1/40 and 1/20 kyr. These last two frequencies are believed to result due to linear response of the climate system to insolation (e.g., Saltzman, 1990; Imbrie et al., 1992, 1993).

The phase locking to Milankovitch is more clearly demonstrated in a model scenario: Suppose we initialize some model of the glacial cycles with different initial conditions for the land ice volume and other variables, and run the model forward in time, simulating glacial cycles. Then all the different initial conditions are influenced by the same external Milankovitch clock, and therefore all of them will adjust their internal oscillation according to the pacing of the external insolation forcing; thus they will converge after some time into a single time series in which the cycles are somehow paced (Hays et al., 1976) by the Milankovitch forcing. This phase locking gives a new meaning to the "pacemaker" idea: Milankovitch forcing is the pacemaker in the sense that glacial cycles are phase-locked to it. Such phase locking is likely the mechanism behind the successful fitting of model results to glacial records, for example by Saltzman (1987) and by Paillard (1998), as these models and the actual ice ages are likely both phase locked to the Milankovitch variations in solar forcing.

Now, the above discussion of phase locking mostly reflects work done on the 100 kyr cycles. The phase locking requires the oscillations to be nonlinear, and the 100 kyr oscillations are indeed both large-amplitude and asymmetric (long glaciation followed by rapid deglaciations), both signs of nonlinearity. It seems that the 40 kyr oscillations are more often thought of as being linearly forced by Milankovitch forcing, especially by obliquity (Raymo and Nisancioglu, 2003; Tziperman and Gildor, 2003).

Clark and Pollard (1998) suggest that the areal extent of the Laurentide ice-sheet was approximately the same before and after the mid-Pleistocene transition, although the maximal ice-volume was larger by a factor of 3/2 during the 100 kyr cycles (assuming the isotopic signal is taken as a mostly ice volume proxy). They therefore propose that the ice-sheet of the 40 kyr glacial cycles was lying on a thin (~ 30 m) deformable regolith layer that could only support a small glacier bottom stress and thus a lower elevation of the ice-sheet (~ 2 km). Successive ice-ages during the 40 kyr glacial oscillations removed the soft layer and uncovered a hard bed-rock that could support a larger bottom stress and a higher elevation ice-sheet (~ 3 km). Based on above Clark and Pollard (1998) developed a ice-flow model to explain the mid-Pleistocene transition. The 40 kyr oscillations in this model are most likely due to Milankovitch variations rather than being self-sustained. That is, the oscillations would not exist without the Milankovitch variations.

Raymo and Nisancioglu (2003) suggested that the northern hemisphere summer insolation gradient (dominated by the obliquity signal) somehow drives the ice-volume variations of the 40 kyr oscillations. However, as we will show below, the insolation gradient is symmetric (increases and decreases in time at the same rate) unlike the ice-ages prior to the mid-Pleistocene transition, which are shown below to be asymmetric. Tziperman and Gildor (2003) tried to attribute the mid-Pleistocene transition to deep ocean cooling, and the 40 kyr oscillations as a linear response to Milankovitch forcing, although their results for the 40 kyr oscillations did not match observations in some critical aspects. Additionally, recent studies (Ruddiman, 2003, 2004) related the mid-Pleistocene transition to a global cooling trend, to linear response to changes in Milankovitch forcing, and to feedback mechanisms related to greenhouse gases. We note that other nonlinear mechanisms (not necessarily self-sustained internal variability) such as (i) different sedimentation rates during glaciation/deglaciation periods or (ii) variable response time that results in a time varying phase of the climate system to Milankovitch forcing, may also produce the asymmetry we observe for the 41 kyr glacial cycles of the mid-Pleistocene.

Nonlinearity does play an important role in some models for the 40 kyr oscillations, even if the oscillations cannot exist without Milankovitch forcing. Examples are the multiple-state model of Paillard (1998), where the mid-Pleistocene transition was simulated by assuming a gradual increase in the maximal ice-volume threshold, and where a good agreement with the proxy records was found. Berger et al. (1999) used the more complex LLN-2D model (Gallée et al., 1991, 1992) with decreasing atmospheric CO_2 in the last 2.7 Ma to simulate the mid-Pleistocene transition. They showed a reasonable agreement with the data. Again, the

oscillations in this model may only exist if Milankovitch forcing is present. Still, nonlinear interactions may, in principle, make the Milankovitch-driven oscillations even before the mid-Pleistocene transition somewhat asymmetric. We note that the obliquity power of glacial cycles pre mid-Pleistocene is similar to obliquity power post mid-Pleistocene while the 100 kyr power is much more pronounced in the past 800 kyr or so. This situation is plausible in both self-sustained mechanism and nonlinear response to Milankovitch forcing scenario.

The objectives of the present study are to show that the 40 kyr glacial oscillations are, in fact, asymmetric and hence to propose that these oscillations are self-sustained nonlinear oscillations rather than a linear response to Milankovitch forcing. We also discuss the possible role of the Milankovitch forcing in affecting the phase and period of the glacial cycles. The highly idealized model we use is derived from the sea-ice-switch model of Gildor and Tziperman (2000) and Tziperman and Gildor (2003). To simulate the mid-Pleistocene transition we use the mechanism of Clark and Pollard (1998) mentioned above.

The paper is organized as followed. In Section 2, we analyze the asymmetry of proxy records of the 40 kyr glacial cycles. In Section 3, we present our ice-ages model and in Section 4, we use the model to discuss the above objectives. We conclude in Section 5.

2. The asymmetry of the 40 kyr glacial oscillations

In this section we analyze the asymmetry of the 40 kyr ice-ages (between 2.5 and 1 Ma ago). We use the time series shown in Fig. 2a, which is a segment of a deep sea Foraminifera $\delta^{18}O$ proxy from site 607 of the Deep Sea Drilling Project (DSDP) (Raymo et al., 1989; Ruddiman et al., 1989), and which is presumably mostly a measure of global ice-volume. The time series was first linearly interpolated to have equal time intervals of 1 kyr between data points. The age model uses no orbital tuning and is constructed by assuming constant sedimentation rates between several known magnetic reversals (see Raymo and Nisancioglu, 2003). While the glacial–interglacial oscillations during 2.5–1Ma ago are apparently symmetric, a closer look shows that most of the ice-ages are asymmetric, with a slow buildup of the ice-sheet that followed by a more rapid melting (some such asymmetric cycles are marked by arrows in Fig. 2). The asymmetry of a time series is stored in the Fourier phases of the series, which contain the information regarding the time direction of the series. It is possible to "destroy" the asymmetry of a time series by randomizing its Fourier phases, leaving the power spectrum and the probability distribution of the time series unchanged (Schreiber and Schmitz, 2000) (see Appendix A for details of the phase randomization procedure). Fig. 2b shows a so-called "surrogate" time series, that is obtained by randomizing the phases of the record shown in Fig. 2a. The probability distribution and the power spectrum of the original data (Fig. 2a) and of the surrogate, phased randomized, time series (Fig. 2b) are identical as expected (Appendix A); see Figs. 2c and d. The surrogate time series are symmetric by construction. Many surrogate time series may be produced from a given time series, and this allows us below to test the statistical significance of our results for the symmetry of the 40 kyr glacial cycles.

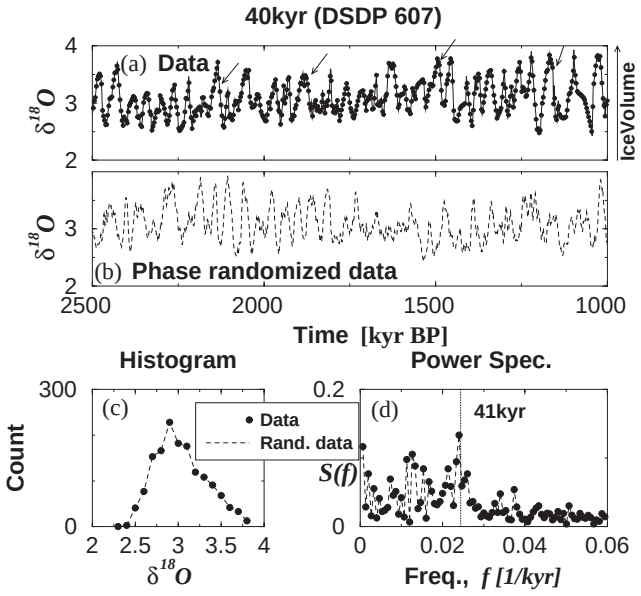

Fig. 2. (a) A segment of the 40 kyr oscillations from the record shown in Fig. 1. The arrows indicate some of the many asymmetric ~ 40 kyr glacial cycles with gradual glaciation followed by more rapid deglaciation. (b) A surrogate series of the segment shown in (a). We destroy the asymmetry of the data by shuffling the Fourier phases, leaving the histogram (c) and the power spectrum (d) of the original data unchanged after the surrogate data test; see text and Appendix Appendix A for more details.

The asymmetry of an evenly sampled time series x_i can be measured as follows. Define an l-size increment of the time series to be $(x_{i+l} - x_i)$. Count now the number of positive increments versus the number of negative increments of the time series for different sizes l. If the positive to negative ratio, p/n, is larger than one then the series generally increases gradually and decreases rapidly. Fig. 3a shows the positive to negative ratio of the 40 kyr data shown in Fig. 2a as well as the p/n ratio of ten phase randomized, symmetric, surrogate time series. The p/n ratio of the data is significantly larger than one while the p/n ratio of the surrogate (symmetric) time series is scattered around one. The asymmetry ratio p/n of the data is clearly above the 90% confidence level since it is located well outside the range of the p/n ratio of the ten surrogate data.

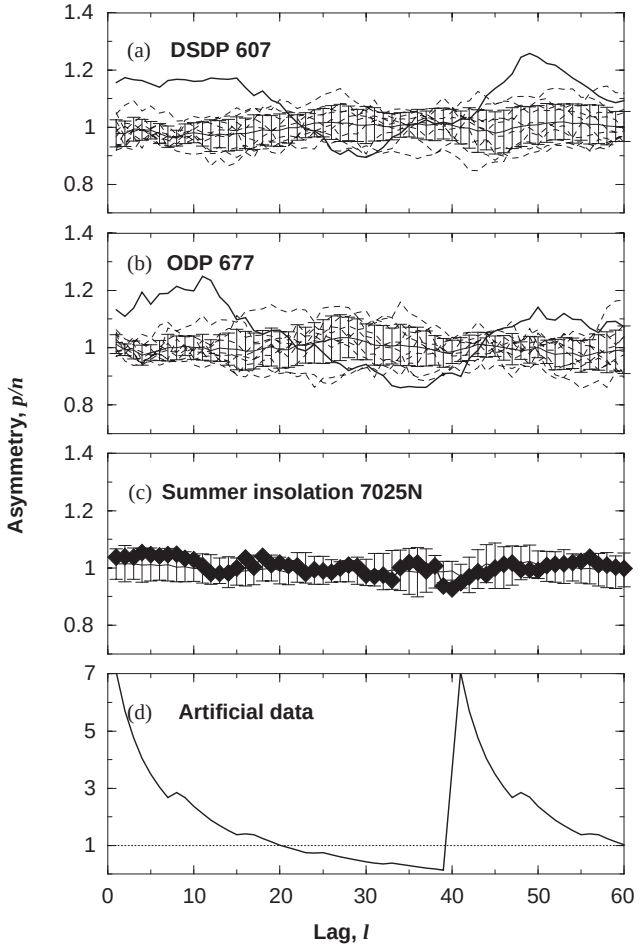

Fig. 3. (a) The asymmetry of the 40 kyr oscillations proxy record (DSDP 607 shown in Fig. 2a), calculated as the ratio between the positive increments and the negative increments for different time lags (solid line, see text for details). The same analysis for ten symmetric, surrogate phase randomized series is shown by dashed lines. The asymmetry in the proxy time series is clearly statistically significant as shown by the comparison with the surrogate data. The asymmetry of the data is well outside the shown vertical bars (marking mean ± 1 standard deviation of the surrogate data) and outside the range of the 10 surrogate data, indicating 90% confidence level. Thus, the 40 kyr ice-ages are clearly asymmetric. (b) Same as (c) for ODP 677. (c) The same analysis applied to the average meridional gradient summer insolation shows that this obliquity-dominated signal is symmetric. Thus, the 40 kyr ice ages cannot be the result of a linear response to Milankovitch forcing. (Insolation (Laskar, 1990; Paillard et al., 1996) is averaged between the vernal and autumnal equinoxes, and the gradient is calculated as the difference between 70°N and 25°N. An analysis of the July 65°N insolation of Berger and Loutre (1991) shows similar results.) (d) The asymmetry of an idealized sawtooth time series that is linearly increasing for 35 kyr and decreasing for 5 kyr. The p/n ratio for lag 1 is 7, representing the ration between increasing time of 35 kyr and the decreasing time of 5 kyr. See text for details.

Thus, in the 40 kyr oscillations the ice-sheet buildup gradually and melts more rapidly, similar to the ice-ages of the past 0.8 Ma. The p/n ratio also reflects the periodicity of the data since for time lags larger than half a period (for the 40 kyr ice ages, half a period is about 20 kyr) the ratio becomes smaller than one. We repeated the analysis for an additional record [Ocean Drilling Project (ODP) Site 677 (Shackleton et al., 1990)] and obtained similar results (Fig. 3b); the chronology that we use is based on a constant sedimentation rate assumption (4.24 cm/kyr) for the past 2.5 Ma.

A previous study (Raymo and Nisancioglu, 2003) suggested that the 41 kyr oscillations are driven by the variations in the northern hemisphere summer insolation gradient due to obliquity changes. We calculate the asymmetry ratio p/n for the insolation gradient presented in Raymo and Nisancioglu (2003) and find that it is symmetric (Fig. 3c). Tziperman and Gildor (2003) also suggested that the 41 kyr oscillations may be linearly driven by the standard 65°N July insolation, yet we find this insolation time series to be symmetric as well.

Fig. 3d shows the positive to negative ratio of an idealized sawtooth time series (increasing linearly for 35 kyr and decreasing linearly for 5 kyr). This figure shows that indeed the p/n ratio reflects the asymmetry of the series, since for lag $1=1$ $p/n=7$ while the ratio between the increasing times and decreasing times is $35/5=7$. The p/n ratio is periodic in the lag, as the sawtooth time series itself, and it becomes smaller than 1 for lags higher than 20 kyr (half of the period).

It should be re-emphasized that given a symmetric Milankovitch forcing, a linear climate dynamics must result in symmetric climate signal. Given our finding above that the 41 kyr oscillations are significantly asymmetric, we thus conclude that ice-ages pre-mid-Pleistocene transition cannot be the result of a direct linear response to the insolation forcing. Our results suggest that ice-ages dynamics pre- and post-mid-Pleistocene transition may both be due to self-sustained nonlinear variability which is indeed typically asymmetric. If this is the case, then the 40 kyr oscillations would have existed regardless of the Milankovitch forcing. Admittedly, having asymmetric oscillations does not rule out the scenario in which the 40 kyr ice ages are not self sustained, but rather are forced by Milankovitch variations in the insolation, and made asymmetric by some nonlinear ice sheet or climate feedbacks.

As will be shown below using a simple model, Milankovitch forcing may still play an important role in our proposed self-sustained glacial oscillations, in setting the phase and affecting the period of the oscillations during both the 40 and 100 kyr ice ages. We finally note that (i) Hagelberg et al. (1991) and (ii) King (1996) demonstrated that the asymmetry of the ice-ages increased drastically after the mid-Pleistocene transition. (iii) Raymo (1992) inspected for DSDP 607 $\delta^{18}O$ that "after 2.2 Ma, rates of ice sheet decay almost always exceed rates of ice growth for a given glacial-interglacial cycle." (iv) Zhonghui and Herbert (2004)

reconstructed the SST of eastern equatorial Pacific and pointed out the asymmetry of the temperature signal during the glacial cycles even before the mid-Pleistocene transition.

3. The model

We now use a simple model in order to examine the possibility that self-sustained glacial oscillations are responsible for the asymmetric 40 kyr oscillations, and to study the possible role of Milankovitch forcing. For this purpose, we simplify the sea ice switch model of Gildor and Tziperman (2000) and Tziperman and Gildor (2003), although the point we wish to make here is independent of the sea ice switch mechanism. We refer the reader to the above papers for a detailed justification of the model assumptions used below.

Assume changes to northern hemisphere ice-volume V to be due to the difference between net snow precipitation over land P and total ablation S (melting, ice-sheet surges, wind erosion etc.); ablation is assumed to depend only on Milankovitch summer radiation at 65°N, so that it equals $S + S_M I(t)$, where $I(t)$ is the July insolation at 65°N (Berger and Loutre, 1991) normalized to zero mean and unit variance and S_M is a constant.

We also assume that precipitation rate P is small for large ice-volume and large for small ice-volume. This is due to the temperature precipitation feedback: as ice sheets grow, their albedo effect cools the atmospheric temperature, and therefore reduces accumulation rate. A simple formulation of accumulation reducing with ice volume is of the form $P(\text{no sea ice}) = p_0 - kV$, where p_0 and k are constants: p_0 is the precipitation rate when the ice-sheets are completely melted and k is the growth rate constant of the ice-sheet.

Following Gildor and Tziperman (2000) we assume that when the ice-volume reaches a certain specified maximal ice-volume V_{max}, the atmospheric temperature becomes sufficiently low such that a significant sea-ice cover rapidly forms. Precipitation over land ice then reduces very sharply because (i) drop in temperature due to the increased albedo of the sea-ice, (ii) reduced evaporation due to insulating sea-ice cover, and (iii) the storm track is shifted by the sea ice away from the ice-sheet. Thus accumulation in the presence of sea ice may be written as $P(\text{with sea ice}) = (p_0 - kV)(1 - a_{si-on})$ where a_{si-on} is the relative area of the sea ice when "on". This reduced accumulation in the presence of sea ice results in land ice withdrawing. When land ice-volume drops below a certain minimal ice-volume V_{min} (resulting in warming due to ice albedo feedback) the sea-ice melts rapidly and precipitation returns to its original rate without sea ice.

Finally, combining the above expressions for the ablation and accumulation, the ice-volume mass balance may be written as

$$\frac{dV}{dt} = (p_0 - kV)(1 - a_{si}) - S - S_M I(t), \quad (1)$$

where a_{si} is the relative area of the sea-ice ($a_{si} = a_{si-on} > 0$ when sea-ice is "on" and $a_{si} = 0$ when sea-ice is "off").

A technical point regarding the model nonlinearity may be due now. Eq. (1) seems linear in the ice volume V. However, because of the dependence of the sea ice area a_{si} on the ice volume at the two threshold points V_{max} and V_{min}, the model is, in fact, nonlinear. The nonlinearity is represented in this "piecewise linear" formulation, where the nonlinearity only occurs at two points. In any case, the model solution below shows self-sustained oscillations which are only possible in nonlinear models (Fig. 4). Appendix B briefly explains the difference between self-sustained, nonlinear, and linear oscillations in the present context.

We note that the model ignores the red spectrum of the climate records (Kominz and Pisias, 1979; Pelletier, 1997; Ashkenazy et al., 2003; Wunsch, 2003) which implies that noise must play an important role. Such noise may be added to this model, yet is not needed for making our main point here.

There are seven parameters for the model (1): V_{min}, V_{max}, a_{si-on}, p_0, k, S, and S_M (Table 1). However, it is possible to switch to normalized ice-volume units without changing the model's dynamics (e.g. by dividing V by V_{min}). This leaves six independent model parameters.

The minimal ice-volume threshold is approximated by $V_{min} = 3 \times 10^6\,km^3$ which is approximately the present day northern hemisphere ice-volume (Hartmann, 1994). The maximal ice-volume is set to $V_{max} = 45 \times 10^6\,km^3$; the total ice-volume increase during the last glacial maximum is $\approx 50 \times 10^6\,km^3$ (Mix et al., 2001) and we assume that most of it ($42 \times 10^6\,km^3$) accumulated in the northern hemisphere ice-sheets and the rest ($8 \times 10^6\,km^3$) in the southern hemisphere ice-sheet and

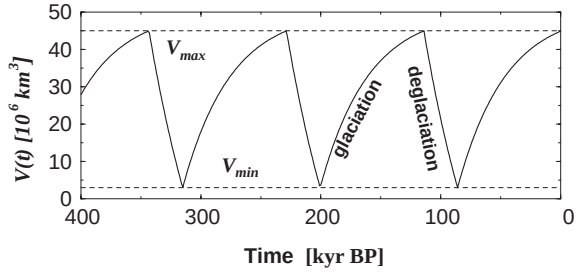

Fig. 4. A time series of the model's ice volume without Milankovitch insolation forcing. The ice volume, $V(t)$, grows when sea-ice cover is absent, till it reaches a maximal threshold V_{max}. Then the sea-ice cover is assumed to be extensive, and the land ice retreats due to ablation until it reaches the minimal ice volume threshold V_{min}.

Table 1
Model's parameters

Parameter	Short description	Value
V_{min}	Minimum ice-volume threshold	3×10^6 km^3
V_{max}	Maximum ice-volume threshold for last 0.81 Ma	45×10^6 km^3
	Maximum ice-volume threshold for 3–1 Ma ago	28×10^6 km^3
k	Ice-sheet constant growth rate	1/40 kyr
p_0	Precipitation rate	0.25 Sv
S	Constant ablation rate	0.21 Sv
S_M	Milankovitch ablation constant	0.023 Sv
a_{si-on}	Relative sea-ice area	0.3

in mountain glaciers. Following Gildor and Tziperman (2000) and Tziperman and Gildor (2003) we choose the relative sea-ice area to be $a_{si-on} = 0.3$. Following Pelletier (1997) and Imbrie and Imbrie (1980) we choose a ice-volume growth rate constant to be $1/k = 40$ kyr. We choose $p_0 = 0.25$ Sv, $S = 0.21$ Sv, and $S_M = 0.023$ Sv, values which are close to the values of Tziperman and Gildor (2003).

4. The mid-Pleistocene transition and role of Milankovitch forcing

Using the simple model presented in the previous section, we wish to now make two main points. First, we will try to show that the 41 kyr oscillations of the mid-Pleistocene may be described as self-sustained oscillations, consistent with their asymmetry discussed in Section 2. Second, we would like to demonstrate that Milankovitch forcing can set the phase of the oscillations, as well as strongly affect and even stabilize the period of the glacial cycles with respect to changes in various external parameters. Our mechanism for the mid-Pleistocene transition itself is based on the "pancake ice sheet" theory of Clark and Pollard (1998).

4.1. Self-sustained 40 kyr glacial oscillations

Clark and Pollard (1998) suggested that prior to the mid-Pleistocene transition, the north American continent was covered by a few tens of meters of regolith which was eliminated by repeated 40 kyr glaciations. The regolith layer can support a smaller horizontal stress by the ice sheet and therefore resulted in a thinner ice sheet. It is fairly simple to incorporate the Clark and Pollard (1998) idea into our model. The maximal ice-volume V_{max} specified as one of the parameters in our model is, in fact, a function of the maximum stress that may be supported at the bottom of the ice sheet. Under the assumption of perfect plasticity, the ice sheet height $h(y)$ is characterized by the so-called parabolic profile (Weertman, 1976; Ghil, 1994) whose height and hence volume depends on the maximum allowed bottom stress.

Note that the maximal area of the ice sheet is determined in our model by its impact on climate via the albedo effect. The land ice area grows until its area and therefore albedo are such that climate cools sufficiently to form sea ice. Thus, according to this scenario (and hence, according to the scenario of Clark and Pollard, 1998) the oscillations in temperature before the mid-Pleistocene transition are expected to be roughly of the same magnitude as those of the 100 kyr oscillations. In fact, a recent study (Zhonghui and Herbert, 2004) presented data that indicates that Equatorial temperature oscillations (Eastern Pacific) pre- and post-mid-Pleistocene transition have roughly the same amplitude variation.

Recent indications are that about half of the benthic δ^{18}O signal during the 100 kyr cycles is due to temperature and half due to ice volume effects (Schrag et al., 1996). If the 40 kyr ice volume oscillations are 2/3 of those during the 100 kyr ice ages, yet the temperature variations are the same, this requires the ratio of ice volume to temperature effects to be different during the 40 kyr ice ages. This raises some interesting questions: did the fraction of the isotopic signal related to temperature change vary during the mid-Pleistocene transition? Why and in what way? It is not clear how to address these questions given present uncertainty in proxy records from the early Pleistocene.

We wish to emphasize that the main point of this work is not that the sea ice switch mechanism applies to the 40 kyr glacial cycles, but rather that these cycles are well described as a self-sustained variability of the climate system (although we cannot rule out the alternative possibility of nonlinear response to Milankovitch forcing). Other model equations that result in self-sustained variability are likely to fit the record as well. The role of Milankovitch forcing discussed later again does not depend on the details of the model used here, and should work equally well for other models with self-sustained oscillations.

Now, we assume that the change in the regolith layer resulted in a change to the maximum supportable bottom stress. This implies that the maximal possible land ice-volume therefore changed linearly from $V_{max} = 28 \times 10^6$ km^3 at 1 Ma ago, to $V_{max} = 45 \times 10^6$ km^3 0.81 Ma ago. All the other parameters are as in Table 1. Fig. 5a shows the (normalized) model's simulation together with benthic δ^{18}O from DSDP607 (again, not orbitally tuned, as explained above). The qualitative correspondence between the model and data is reasonable, and is even better when considering the shorter interval of 0.5–0 Ma ago. Table 2 summarizes the correlation coefficients of different time periods shown in Fig. 5 (2.5 Ma ago to present, 1.6–1 Ma ago, and

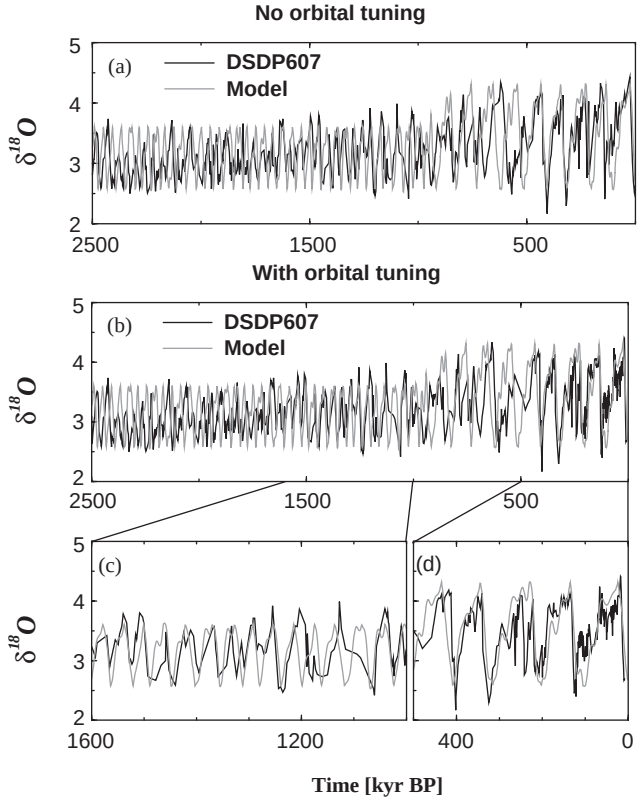

Fig. 5. (a) A simulation of the mid-Pleistocene transition. The model is run with Milankovitch forcing (65°N July insolation) for the past 3 Ma. Motivated by proxy observations, the maximal ice volume threshold before 1 Ma ago is set to $\sim 2/3$ of the maximal ice volume of the last 0.8 Ma; i.e., $V_{\max} = 28 \times 10^6\,\mathrm{km}^3$ before 1 Ma ago, increases linearly to $V_{\max} = 45 \times 10^6\,\mathrm{km}^3$ at 0.81 Ma ago and remain constant later on. A proxy record that is not orbitally tuned (DSDP 607, black curve) is shown with the normalized model data (gray curve). (b) Same as (a) but for orbitally tuned chronology (Raymo et al., 1989; Ruddiman et al., 1989). Here the agreement between the data and the model is better than for the non-orbitally tuned data, most probably due to the calibration of the data with Milankovitch forcing. (c) Enlargement of a segment (1.6–1 Ma ago) from the 40 kyr oscillation era shown in (b). (d) Enlargement of a segment from the 100 kyr oscillations (the last 0.5 Ma) shown in (b). The correlation coefficients between the data and the model are summarized in Table 2.

Table 2
A summary of the correlation coefficients between the data (DSDP 607 and ODP 677) and the model as shown in Fig. 5a

	2.5–0 Ma ago	1.6–1 Ma ago	0.5–0 Ma ago
DSDP607 vs. Model	0.26 (0.39)	0.11 (0.47)	0.62 (0.64)
ODP677 vs. Model	0.23 (0.53)	0.12 (0.57)	0.33 (0.73)
DSDP607 vs. ODP677	0.36 (0.67)	−0.1 (0.73)	0.51 (0.73)

The value in brackets are the correlation coefficients for the orbitally tuned records ODP 677 (Shackleton et al., 1990) and DSDP 607 (Ruddiman et al., 1989; Raymo et al., 1989) (shown in Figs. 5b–d); these values indicate better correspondence between the data and the model, most probably due to phase-locking to Milankovitch.

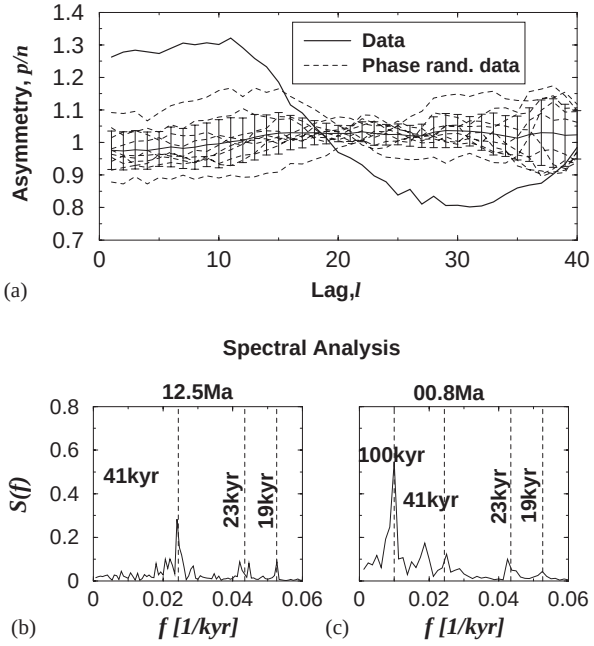

Fig. 6. (a) Analysis of the asymmetry of the model's ice volume time series from 2.5 to 1 Ma ago, shown in Fig. 5. The asymmetry of the model's ice volume is similar to the asymmetry curve obtained from the data (Figs. 3a and b). The asymmetry of the model is again significantly different from that of the symmetric surrogate data, indicating that the model's ice volume signal is indeed asymmetric. (b) Power spectrum of the model's ice volume time series shown in Fig. 5 for the time period 2.5–1 Ma ago. The pronounced peak of 41 kyr is associated with the obliquity frequency and the 23 and 19 kyr secondary peaks are associated with the precessional frequency. (c) Same as (b), but for the past 0.8 Ma. Here, the most dominant frequency of 100 kyr is due to the self-sustained internal model dynamics. The obliquity and precession frequencies are still present, but are less pronounced.

0.5 Ma to present). The relatively good correspondence between the model results and the 40 kyr glacial cycles is supplemented by the reasonable 100 kyr cycles after the mid-Pleistocene transition, created due to the specified increase in the parameter $V_{\max}$.

In Fig. 5b we plot the orbitally tuned data versus the model's output. Here, the agreement between data and model is significantly better. We summarize the correlation coefficients of the different segments of the data in Table 2 values in brackets. This better agreement suggests that if indeed Milankovitch forcing influences the glacial–interglacial oscillations it is through the phase-locking mechanism. Unfortunately, the current precision for the dating of the proxy records does not allow to accurately determine the role of Milankovitch forcing on the timing of the ice-ages.

In any case, our objective here is not to present (yet another) good fit to proxy records. We do wish to make the point that the asymmetry of the self-sustained model oscillations prior to the mid-Pleistocene transition is similar to that of the observed proxy record (Fig. 6). We

wish to use this similarity to motivate our suggestion that the 40 kyr oscillations may have been self-sustained oscillations rather than a linear response to Milankovitch forcing. In Fig. 6a we show the asymmetry analysis (previously performed on the observations in Section 2, Fig. 3). Similarly, the spectrum for the 40 kyr oscillations is similar for the model and observations (Figs. 6b and c). Specifically, the ratio of the orbital frequencies of obliquity and precession are similar. Next, we discuss the role of Milankovitch forcing in these self-sustained oscillations.

4.2. Milankovitch forcing: phase locking and possible stabilization of glacial period

Proceed now to the role of Milankovitch forcing. Gildor and Tziperman (2000) demonstrated that the Milankovitch forcing sets the phase of the 100 kyr glacial cycles, and this was previously also hinted by Saltzman (1987) and Raymo (1997). This phase locking to Milankovitch is demonstrated in Fig. 7. We run the model for six different initial conditions (starting 3 Ma ago) for the land ice volume, ranging from $V_{\min}$ to $V_{\max}$. After few 40 kyr glacial cycles, the different curves converge to single curve (Fig. 7). Without the isolation forcing the different curves would keep their different initial relative phases forever. Thus we would like to make the point that the 40 kyr oscillations may again be self-sustained oscillations phase locked to Milankovitch, as seems to be the case for the 100 kyr ice ages.

Fig. 7 also shows the 65°N July insolation of Berger and Loutre (1991). The model's deglaciations tend to start when insolation is close to minimum (Gildor and Tziperman, 2000). This is because at times of minimum insolation, ablation is low, land ice tends to grow faster and reach the critical threshold at which sea ice forms and termination starts. Since the minimum points of insolation are dominated by precession, they will occur every ~ 20 kyr. Thus, we expect the glacial-interglacial oscillation period to be a multiple of the precession frequency (Raymo, 1997; Ridgwell et al., 1999). However, as explained above, this need not always be the case, as deglaciations do not exactly start at minimum insolation times even in our simple model, and things are further complicated by the existence of two dominant precession frequencies, and by the presence of noise.

However, there is a further point regarding the role of Milankovitch forcing here, which is demonstrated in Fig. 8. In this figure we plot the period of the model as function of the specified maximum ice volume $V_{\max}$. This is done both with and without Milankovitch forcing, and for forcing using insolation gradient only (dominated by obliquity, Raymo and Nisancioglu, 2003) and using the usual 65°N July insolation. The dashed lines show that the period of the oscillations smoothly increases with $V_{\max}$ when no Milankovitch forcing is

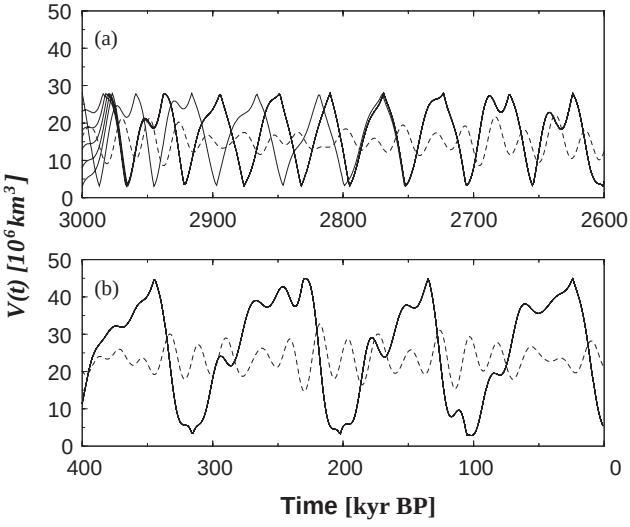

Fig. 7. Segments of the model's ice volume $V(t)$ from the last 3 Ma when the 65°N July insolation of Berger and Loutre (1991) is added to the ablation term. We run the model for six different initial ice volumes [ranging from $V(-3\,\text{Ma}) = V_{\min} = 3 \times 10^6\,\text{km}^3$ to $V(-3\,\text{Ma}) = V_{\max} = 28 \times 10^6\,\text{km}^3$]. After few cycles the different ice volume curves collapse to a single curve (displayed in the upper panel) due to phase locking to the insolation forcing. The dashed line indicates the insolation forcing (in arbitrary vertical scales and offsets) and it seems that deglaciation starts when insolation is minimal. (a) $V(t)$ of the 3–2.6 Ma ago. (b) $V(t)$ of 0.4 Ma ago to present. Note that (b) is showing the final parts of the simulations that their beginnings are shown in (a).

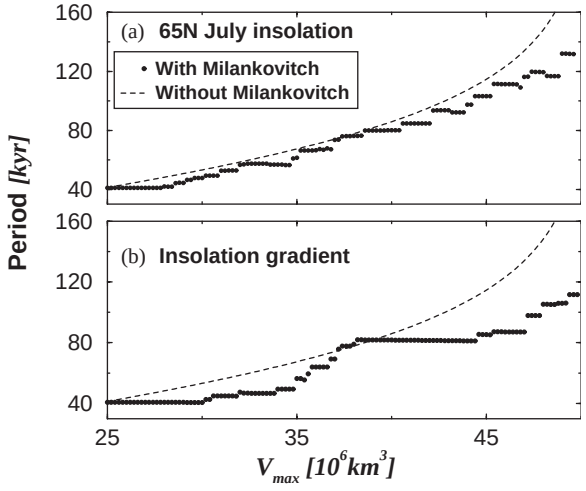

Fig. 8. The average period of the glacial cycles during the past 0.8 Myr as function of the maximum land ice volume specified in the model, $V_{\max}$. The dotted (dashed) lines show the period as function of $V_{\max}$ with (without) Milankovitch forcing. Upper panel: Milankovitch forcing is the July radiation at 65°N (Berger and Loutre, 1991). Lower panel: the gradient of the June 21st insolation from 70°N to 25°N (which is dominated by the obliquity signal) is used as Milankovitch forcing (based on Laskar, 1990).

applied. However, when Milankovitch forcing is present, there are fairly large regimes in which the period does not change in spite of the changes to $V_{\max}$. Note that the average period is shown, while individual glacial periods are scattered around the average value. The robustness of the period with respect to $V_{\max}$ is especially evident when forcing the model with the obliquity dominant signal (Fig. 8b). The model clearly tends to oscillate at multiples of the obliquity frequency, either 40 or 80 kyr, with a relatively small transition region between them (i.e. small range of $V_{\max}$ in which the period is not a multiple of 40 kyr). This is a by-product of the phase locking seen by the convergence of the runs with different initial conditions seen in Fig. 7. What Fig. 8 shows is that the average frequency of the glacial cycles is made more robust because of the phase locking to the Milankovitch forcing. That is, even if some external conditions slowly change (e.g. CO_2 concentration), the oscillation frequency tends to be robust and vary only in jumps once the change to the external conditions has accumulated significantly. However, since one expect that both the local insolation as well as the insolation gradient to play an important role on glaciation dynamics, the upper panel of Fig. 8 seems to be more realistic. Now, when forcing the model with the 65°N insolation, the discrete jumps in the period as function of $V_{\max}$ are less pronounced, because of the shorter period of the precession-dominated forcing and because of the presence of several precession frequencies (19 and 23 kyr) etc.

The roughly 20 kyr precession peaks of insolation have different amplitude depending on the eccentricity, and especially weak peaks tend to occur every about 100 kyr (and even more so every 400 kyr). Raymo (1997) and Ridgwell et al. (1999) suggested that deglaciation starts after these especially low precession insolation peaks, because such low peaks allow for land ice growth and lead to ice sheet instabilities and to terminations. However, this scenario doesn't seem to fit the ice-ages of the pre-mid-Pleistocene period, where terminations occurred roughly every 40 kyr, and hence necessarily could not be correlated with low precession peaks which occur every 100 kyr. In any case, our model does not seem to respond in a special way to the variations in the amplitude of the eccentricity peaks.

Now, the Milankovitch forcing amplitude in the ablation term (1) is only about 10% of the other ablation/accumulation terms, i.e. 10% of $(p_0 + S)/2$ (equivalently, the Milankovitch forcing is 14% of $(p_0 - kV)(1 - a_{\mathrm{si-on}})$ using an average ice-volume value of $V = 20 \times 10^6\,\mathrm{km}^3$). The above results suggest that even relatively small contribution of the insolation forcing may have an important role on the timing and period of the ice-ages. Moreover, the insolation forcing results in a unique curve for ice-volume that can be compared to the observed data. Demonstrating a good correspondence between paleoclimate records (that are not orbitally tuned) and models that are phased locked to insolation variations may help to quantify how significant is the influence of insolation variations on climate.

5. Conclusions

It is often stated that the 40 kyr glacial cycles prior to the mid-Pleistocene transition are a linear response to Milankovitch forcing. We showed here that the 40 kyr oscillations are significantly asymmetric, having longer glaciations than deglaciations, similarly to, although not as pronounced as, the asymmetry of the 100 kyr oscillations. Such asymmetry is a clear signature of nonlinearity.

There are two main alternative suggestions for the character of glacial cycles. The first is that these cycles are a response (linear or nonlinear) to Milankovitch forcing. This implies that the cycles would not have existed without the orbitally caused variations to the solar insolation. The second is that the glacial oscillations are due to the internal dynamics of the climate system and would have existed even without the Milankovitch forcing. The nonlinear oscillations, according to this scenario, are also often termed "self-sustained" for this reason. The role of the orbital forcing in this second scenario is in possibly setting the phase (timing) of the glacial oscillations. An additional alternative is that the oscillations would not have existed without the Milankovitch forcing, yet that some thresholds exist in the climate system that modulate the climate response to Milankovitch (Imbrie and Imbrie, 1980; Paillard, 1998). These thresholds can introduce asymmetry into the climate response, resulting in the observed asymmetric glaciation. Differentiating between these scenarios for both the 100 kyr oscillations, and the 40 kyr oscillations is clearly an important and interesting goal. The present study can merely raise the possibility of self-sustained mechanism, and cannot rule out alternatives such as nonlinear response to Milankovitch forcing.

We analyzed glacial proxy records for the 40 kyr ice ages before the mid-Pleistocene transition, and found them to be significantly asymmetric. We explained that this rules out the possibility that these oscillations are a purely linear response to Milankovitch forcing. We used a highly idealized model to demonstrate that explaining the 40 kyr ice ages as self-sustained nonlinear oscillations results in an asymmetry of the ice volume record which is consistent with the observed asymmetry. We further demonstrated the two roles of Milankovitch forcing. The first role is to set the phase of the oscillations via what's known as a "nonlinear phase locking". We feel that this phase locking is an appropriate specific physical mechanism for the

common and somewhat more vague suggestion that Milankovitch forcing is the pacemaker of glacial cycles (Hays et al., 1976). The second role of the Milankovitch forcing demonstrated here is in the stabilization of the glacial period to slow changes (such as changes to the bedrock or atmospheric CO_2). The model used here displays nonlinear self-sustained oscillations, that are also forced (externally) by Milankovitch forcing. This oscillations may exist even without the Milankovitch variations, yet these variations "pace" (via nonlinear phase locking) the self sustained oscillations due to the internal climate variability.

Raymo and Nisancioglu (2003) proposed that the insolation gradient has a dominant effect on ice-ages of the 40 kyr oscillations, because the insolation gradient is dominated by the obliquity signal. We cannot rule out a dominant role for the insolation gradient, although our results imply that the 40 kyr cycles are not a linear response to obliquity forcing. It is possible that the insolation gradient somehow phase locks a nonlinear oscillation during the 40 kyr ice ages.

The model presented in this paper is clearly highly simplified and excludes many important physical processes; clearly it would be desirable to use a more complex model to look into these issues. However, the main point of this work does not depend on the details of the specific simple model we have used. The robust message of this paper is that we have demonstrated that the 40 kyr oscillations are significantly asymmetric and may not be explained as a linear response to Milankovitch forcing. These cycles may therefore be self-sustained oscillations, as the 100 kyr oscillations are commonly believed to be.

Acknowledgements

ET is supported by the McDonnell Foundation. We thank Hezi Gildor and Peter Stone for helpful discussions, and to two anonymous reviewers for their helpful comments.

Appendix A. Phase randomization

Given a time series h_k with a sampling rate Δ, it is possible to perform a Fourier transform in order to find the frequency spectrum of the series. The Fourier transform results in a complex Fourier series $H_n \equiv A_n \exp[i\varphi_n]$ where A_n is the Fourier amplitude and φ_n is the phase. The relation between the original series h_k and Fourier series H_n is

$$H_n \equiv \Delta \sum_{k=0}^{N-1} h_k e^{2\pi i k n/N}$$

and

$$h_k \equiv \frac{1}{N\Delta} \sum_{n=0}^{N-1} H_n e^{-2\pi i k n/N},$$

where N is the number of data points of the time series h_k.

Now, the information regarding the "time direction" of the time series h_k if stored in the Fourier phases φ_n—when, e.g., one inverts the direction of the time series h_k by changing Δ to $-\Delta$ just the phase φ_n changes to $\varphi_n + \pi$ while the Fourier amplitude A_n remains unaffected. The asymmetry of h_k is an indication for the time direction of the series and is reflected in the Fourier phases φ_n. Thus, if one would like to "destroy" the asymmetry of the time series h_k he should first perform a Fourier transform, then replace the phases φ_n by uniformly distributed random phases and then perform an inverse Fourier transform. The resulting series should not contain any information regarding the time direction of the original series. It is known however that this procedure may alter the original probability distribution of h_k; one would prefer to keep the original distribution of the time series unchanged after randomizing the Fourier phases in order to preserve as much knowledge as possible of the original time series.

Schreiber and Schmitz (2000) suggested an algorithm which preserves both the original probability distribution of the time series as well as its Fourier amplitudes but randomizes the Fourier phases. The algorithm is an iterative algorithm and consists of the following steps:

(i) Store a sorted list of the original data $\{h_k\}$ and the power spectrum $\{S_n\}$ of $\{h_k\}$.
(ii) Begin ($l = 0$) with a random shuffle $\{h_k^{(l=0)}\}$ of the data.
(iii) Replace the power spectrum $\{S_n^{(l)}\}$ of $\{h_k^{(l)}\}$ by $\{S_n\}$ (keeping the Fourier phases of $\{S_k^{(l)}\}$) and then transform back.
(iv) Sort the series obtained from (iii).
(v) Replace the sorted series from (iv) by the sorted $\{h_k\}$ and then return to the pre-sorting order [i.e., the order of the series obtained from (iii)]; the resulting series is $\{h_k^{(l+1)}\}$.

Repeat steps (iii)–(v) until convergence (i.e., until series from consecutive iterations will be almost the same)

In order to check if a time series is symmetric or asymmetric it is possible to generate many surrogate symmetric time series out of the original time series and then to check how significant is the asymmetry of the original time series compare to the asymmetry of the surrogate (symmetric) time series.

Appendix B. Linear, nonlinear and self-sustained glacial oscillations

B.1. Linear oscillations

A basic equation for linear oscillations is the harmonic oscillator $d^2x/dt^2 + x = 0$. The amplitude of the oscillations of a harmonic oscillator depend on the initial conditions; i.e., different initial conditions will lead to oscillations with different amplitudes proportional to the amplitude of the initial conditions. When forced by an external periodic forcing (e.g. Milankovitch forcing), with a frequency different from the natural frequency and damped by friction, the oscillation amplitude will be proportional to the amplitude of the external forcing.

B.2. Nonlinear self-sustained oscillations

Suppose now that we add a nonlinear term to the harmonic oscillator to get the van Der Pol oscillator, $d^2x/dt^2 - \varepsilon(1 - x^2)dx/dt + x = 0$. When $\varepsilon \ll 1$ one obtains a periodic solution (for $t \gg 0$) which is *independent* of the initial conditions and results in a single unique curve in the phase space. I.e., $x(t) = 2\cos t$ and $dx/dt = -2\sin t$. These are self-sustained oscillations (although only weakly nonlinear), and this is what is referred to in the text of this paper as self-sustained oscillations, requiring no external forcing to be sustained. When $\varepsilon \gg 1$ the oscillations are also periodic and self-sustained but strongly nonlinear with sharp transitions (fast and slow phases); these are *relaxation oscillations* (Strogatz, 1994), which are the class of self-sustained oscillations perhaps the most relevant to glacial cycles. The power spectrum of such oscillations shows the basic frequency of the system with several strong harmonics.

References

Ashkenazy, Y., Baker, D.R., Gildor, H., Havlin, S., 2003. Nonlinearity and multifractality of climate change in the past 420,000 years. Geophysical Research Letters 30 (22), 2146 (10.1029/2003GL018099).

Berger, A., Loutre, M.F., 1991. Insolation values for the climate of the last 10 million years. Quaternary Science Review 10, 297–317.

Berger, A., Li, X., Loutre, M., 1999. Modelling northern hemisphere ice volume over the last 3 Ma. Quaternary Science Review 18, 1–11.

Clark, P.U., Pollard, D., 1998. Origin of the middle Pleistocene transition by ice sheet erosion of regolith. Paleoceanography 13 (1), 1–9.

Gallée, H., vanYpersele, J., Fichefet, T., Tricot, C., Berger, A., 1991. Simulation of the last glacial cycle by a coupled sectorially averaged climate-ice sheet model. 1. The climate model. Journal of Geophysical Research 96, 13,139–13,161.

Gallée, H., vanYpersele, J., Fichefet, T., Marsiat, I., Tricot, C., Berger, A., 1992. Simulation of the last glacial cycle by a coupled sectorially averaged climate-ice sheet model. 2. Response to insolation and CO_2 variations. Journal of Geophysical Research 97, 15,713–15,740.

Ghil, M., 1994. Cryothermodynamics: the chaotic dynamics of paleoclimate. Physica D 77, 130–159.

Gildor, H., Tziperman, E., 2000. Sea ice as the glacial cycles climate switch: role of seasonal and orbital forcing. Paleoceanography 15, 605–615.

Hagelberg, T., Pisias, N., Elgar, S., 1991. Linear and nonlinear couplings between orbital forcing and the marine $\delta^{18}O$ record during the late Neogene. Paleoceanography 6 (4), 729–746.

Hartmann, D., 1994. Global Physical Climatology. Academic Press, San Diego.

Hays, J.D., Imbrie, J., Shackleton, N.J., 1976. Variations in the earth's orbit: pacemakers of the ice ages. Science 194, 1121–1132.

Imbrie, J., Imbrie, J.Z., 1980. modelling the climatic response to orbital variations. Science 207, 943–953.

Imbrie, J., Boyle, E.A., Clemens, S.C., Duffy, A., Howard, W.R., Kukla, G., Kutzbach, J., Martinson, D.G., McIntyre, A., Mix, A.C., Molfino, B., Morely, J., Peterson, L.C., Pisias, N., Prell, W.L., Raymo, M.E., Shackleton, N.J., Toggweiler, J.R., 1992. On the structure and origin of major glaciation cycles. 1. Linear responses to Milankovitch forcing. Paleoceanography 7, 701–738.

Imbrie, J., Berger, A., Boyle, E.A., Clemens, S.C., Duffy, A., Howard, W.R., Kukla, G., Kutzbach, J., Martinson, D.G., McIntyre, A., Mix, A.C., Molfino, B., Morley, J.J., Peterson, L.C., Pisias, N.G., Prell, W.L., Raymo, M.E., Shackleton, N.J., Toggweiler, J.R., 1993. On the structure and origin of major glaciation cycles. 2. The 100,000–year cycle. Paleoceanography 8, 699–735.

King, T., 1996. Quantifying nonlinearity and geometry in time series of climate. Quaternary Science Review 15, 247–266.

Kominz, M., Pisias, N., 1979. Pleistocene climate—deterministic or stochastic. Science 204, 171–173.

Laskar, J., 1990. The chaotic motion of the solar system: a numerical estimate of the chaotic zones. Icarus 88, 266–291.

Milankovitch, M., 1941. Canon of insolation and the ice-age problem. Royal Serbian Academy, Special Publication No. 132, translated from German by Israel Program for Scientific Translations, Jerusalem, 1969.

Mix, A.C., Bard, E., Schneider, R., 2001. Environmental processes of the ice age: land oceans glaciers (EPILOG). Quaternary Science Reviews 20, 627–657.

Paillard, D., 1998. The timing of Pleistocene glaciations from a simple multiple-state climate model. Nature 391, 378–381.

Paillard, D., 2001. Glacial cycles: toward a new paradigm. Reviews of Geophysics 39, 325–346.

Paillard, D., Labeyrie, L., Yiou, P., 1996. Macintosh program performs time-series analysis. Eos Transactions AGU 77, 379.

Pelletier, J., 1997. Analysis and modeling of the natural variability of climate. Journal of Climate 10, 1331–1342.

Raymo, M.E., 1992. Global climate change: a three million year perspective. In: Kukla, G., Went, E. (Eds.), Start of a Glacial, NATO ASI Series I, Vol. 3. Proceedings of the Mallorca NATO ARW. Springer, Heidelberg, pp. 207–223.

Raymo, M.E., 1997. The timing of major terminations. Paleoceanography 12, 577–585.

Raymo, M.E., Nisancioglu, K., 2003. The 41 kyr world: Milankovitch's other unsolved mystery. Paleoceanography 18 (1), 1011 (doi:10.1029/2002PA000791).

Raymo, M.E., Ruddiman, W.F., Backman, J., Clement, B.M., Martinson, D.G., 1989. Late pliocene variation in northern hemisphere ice sheets and north atlantic deep circulation. Paleoceanography 4, 413–446.

Ridgwell, A.J., Watson, A.J., Raymo, M.E., 1999. Is the spectral signature of the 100 kyr glacial cycle consistent with a Milankovitch origin? Paleoceanography 14, 437–440.

Ruddiman, W.F., 2003. Orbital forcing ice volume and greenhouse gases. Quaternary Science Reviews 22, 1597–1629.

Ruddiman, W.F., 2004. The role of greenhouse gases in orbital-scale climatic changes. EOS 85 (1), 1.

Ruddiman, W.F., Raymo, M.E., Martinson, D.G., Clement, B.M., Backman, J., 1989. Pleistocene evolution: Northern hemisphere ice sheets and North Atlantic Ocean. Paleoceanography 4, 353–412.

Saltzman, B., 1987. Carbon dioxide and the $\delta^{18}O$ record of late-Quaternary climatic change: a global model. Climate Dynamics 1, 77–85.

Saltzman, B., 1990. Three basic problems of paleoclimatic modeling: a personal perspective and review. Climate Dynamics 5, 67–78.

Schrag, D., Hampt, G., Murray, D., 1996. Pore fluid constraints on the temperature and oxygen isotopic composition of the glacial ocean. Science 272, 1930–1932.

Schreiber, T., Schmitz, A., 2000. Surrogate time series. Physica D 142, 346–382.

Shackleton, N.J., Berger, A., Peltier, W.R., 1990. An alternative astronomical calibration of the lower pleistocene time scale based on ODP site 677. Transactions of the Royal Society of Edinburgh: Earth Sciences 81, 251–261.

Strogatz, S., 1994. Nonlinear Dynamics and Chaos. Westview Press, Boulder, CO, USA.

Tziperman, E., Gildor, H., 2003. The mid-Pleistocene climate transition and the source of asymmetry between glaciation and deglaciation times. Paleoceanography 18 (1) (10.1029/2001PA000627).

Weertman, J., 1976. Milankovitch solar radiation variations and ice age ice sheet sizes. Nature 261, 17–20.

Wunsch, C., 2003. The spectral description of climate change including the ky energy. Climate Dynamics 20, 353–363 (doi:10.1007/s00382-002-0279-z).

Zhonghui, L., Herbert, T.W., 2004. High-latitude influence on the eastern equatorial pacific climate in the early Pleistocene epoch. Nature 427, 720–723 (doi:10.1038/nature02338).